The paper was published in the proceedings of the 7th International Conference on Earthquake Geotechnical Engineering and was edited by Francesco Silvestri, Nicola Moraci and Susanna Antonielli. The conference was held in Rome, Italy, 17 – 20 June 2019.

Earthquake Geotechnical Engineering for Protection and Development of Environment and Constructions – Silvestri & Moraci (Eds)
 ISBN 978-0-367-14328-2

Strength-deformation characteristics of short fiber mixed soil for mitigation of liquefaction hazards

K. Sato, T. Fujikawa & C. Koga
Fukuoka University, Fukuoka, Japan

T. Newson
Western University, London Ontario, Canada

ABSTRACT: The Great Eastern Japan Earthquake occurred on March 11, 2011 and caused significant liquefaction damage. Liquefaction occurred in Tohoku and Kanto region. Especially, the damages of houses became a serious problem in Tokyo Bay coastal landfill and Kanto inland area. Liquefaction has been reported that a long earthquake duration time has expanded the liquefaction area. Also, in the survey results after earthquake in Tokyo bay area, the particle size distribution of the sand boiling contained a lot of silt. Therefore, this research is focused on the effect of fiber on liquefaction properties of short fiber mixed soil containing fine fraction. This paper reports the basic liquefaction characteristics of short fiber mixed reinforcement soil method. In particular, the effect of short fiber length and fine fraction content (silt content) on liquefaction characteristics by short fiber mixing is reported.

1 INTRODUCTION

Japan is one of the most earthquake prone countries in the world. Japan is affected by various damaging phenomena, such as liquefaction during earthquakes. The Great Eastern Japan Earthquake, which occurred in 2011, lead to significant earthquake motions, tsunami, liquefaction, fire and nuclear power plant. These hazards occurred very extensively across the region. The ground which sand boiling occurred includes a lot of silt, and it is thought that long duration of ground motion was the cause that raised damage in the ground including a lot of silt (Yasuda et al. 2012, Miwa et al. 2012). The potential for huge earthquake occurrences in Japan is concerned significantly. Accordingly, it is necessary for methods of suppression of liquefaction to be considered for these longer earthquake durations. In the liquefaction countermeasure of the land reclamation, there is the Premixing Method. The premixing method is one of the ex-situ admixture stabilization techniques where a small amount of binder and chemical additives are mixed with sandy material to obtain liquefaction-free material for land reclamation (Zen et al. 1987, Costal Development Institute of Technology, 2003). In this method, the strength and rigidity of the treated soil increase by addition and mixing of cement but do not have toughness. In the long duration earthquake, the toughness of the ground is thought to lead to the reduction of liquefation damage expansion. Therefore, in this study, we focus on short fiber mixed reinforcement soil method that improves mechanical properties such as strength and toughness of soil by mixing short fiber as a tensile reinforcing material in soil. From previous research, the erosion resistance ability based on a long-term field test construction was verified, and addition of strengthening effect and confined effect of toughness were also verified by static and dynamic compression tests (Hirano et al. 2013). Also, previous studies have confirmed toughness and strength increase which are properties that are not easily broken by intertwining soil particles and short fiber (Ibraim et al. 2010, Li et al. 2017, Wood et al. 2016). Furthermore, authors (Nakamichi et al. 2013) confirmed an

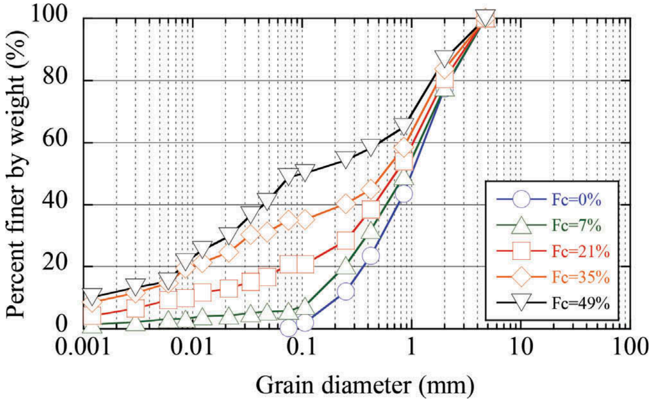

Figure 1. Particle size distribution ofsoil samples.

Table 1. Physical properties of each decomposed granite soil.

Sample	Soil particle density ρ_s (g/cm^3)	Maximum void ratio e_{max}	Minimum void ratio e_{min}	Fine fraction content F_c (%)	Plasticity index I_P
Decomposed granite soil	2.716	1.180	0.616	9	N.P.
Low plasticity fine grained soil	2.790	-	-	64	13.88

increase in liquefaction strength due to short fiber mixing. This paper reports on the effect of fiber length on liquefaction properties of short fiber mixed soil containing fine fraction.

2 TESTING PROCEDURE

2.1 *Soil sample and short fiber*

In this study, a decomposed granite soil was used to investigate the effect of fiber length on liquefaction properties of short fiber mixed soil containing fine fraction. Figure 1 shows the particle size distribution curves of decomposed granite soil. Table 1 shows the physical properties of each decomposed granite soil. Decomposed granite soil was used for the soil sample adjusting the fine fraction content rate at 0, 7, 21, 35, 49 % using reddish soil (silt). PVA fiber of length 12, 40, 60 mm was used as short fiber materials. The fiber is a polyvinyl alcohol fiber which is made by Kuraray Co., Ltd.

2.2 *Preparing method of specimens*

The size of the specimen for the cyclic triaxial test used in the experiment is 75 mm in diameter and 150 mm in height. Specimens were prepared with a target dry density of 1.49 g/cm^3, equivalent to a relative density of D_r =60 % of Toyoura sand (irrespective of the presence or absence of additional cement solidification material). Specimens were prepared using the tamping method.

The low plasticity fine fraction was blended separately outside of the specimen and mixed at various percentages to the absolute dry mass of soil sample. Regulation of the water content was set to 10 % after mixing of the sand and short fiber.

2.3 *Test condition*

This study involves the investigation of liquefaction mechanisms using short fiber mixed soil.

2.3.1 *Effect of short fiber length and fine fraction content*

Table 2 shows the testing conditions. In a series of experiments, when the short fiber content was set to SF= 0 or 1%, the short fiber lengths (L = 12, 40, 60 mm) and fine fraction content (FC = 0, 7, 21, 35, 49 %) was changed. The short fiber are mixed in a length of 0.16, 0.53 and 0.80 times the diameter (ϕ=75mm) of the specimen.

2.3.2 *Testing methods*

The experiments were conducted using undrained cyclic shear test. Undrained cyclic shear tests were carried out under sine-wave stress control with a load speed of 0.1 Hz. The termination condition of this test is when double amplitude of DA=5 % was reached. In addition, all experiments were carried out under an effective confining pressure of 100 kPa and a back pressure of 200 kPa. In addition, the degree of saturation (Skempton's B value) of the specimens in all conditions was more than B=0.96.

2.4 *Relation between skeleton structure of soil andfine fraction content*

The mechanical properties of soil containing fine grains are thought to be the dominant factor of the soil skeleton structure. Therefore, in this research, the state of the particle skeleton was investigated by using the concept of the skeleton void ratio (Yajima et al., 1999). The composition of the soil is divided into three types: sand particles, fine fraction, and voids (Figure 2). The void ratio is obtained from the ratio of the sum of the volumes of sand particles and fine fraction and the

Table 2. Test conditions.

Sample	Short fibers mixing ratio SF (%)	Fiber length L (mm)	Fine fraction content Fc (%)	Target dry density ρd (g/cm^3)	Set water content w (%)
Decomposed granite soil	SF=0%	-	0, 7, 21, 35, 49	1.49	10
	SF=1%	12 40 60	7, 21, 35, 49		

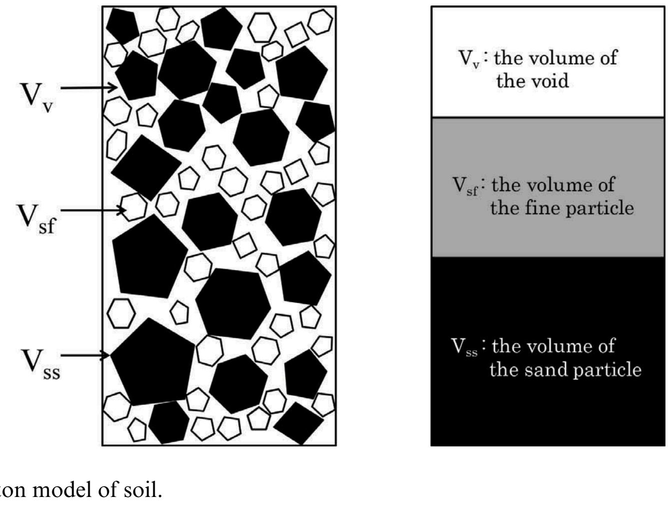

Figure 2. Skeleton model of soil.

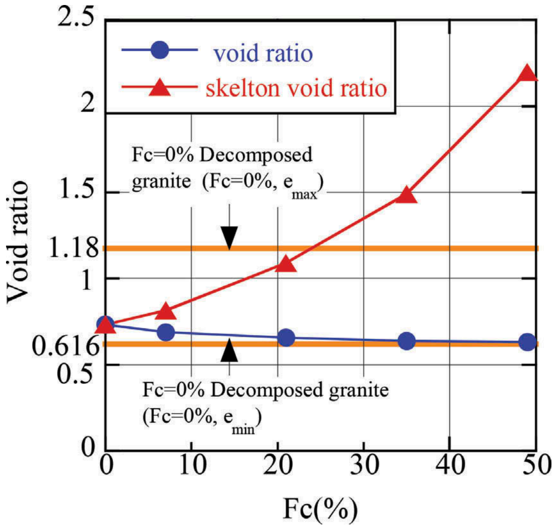

Figure 3. Relationship between void ratio and fine fraction content, Fc (%).

volume of voids, whereas the skeleton void ratio is regarded as the void as well as the volume of fine fraction, and from the ratio of the volume of sand particles to the following formula.

$$e_s = \frac{V_v + V_{sf}}{V_{ss}} \tag{1}$$

Here, e_s is the skeleton void ratio, V_v is the volume of the void, V_{sf} is the volume of the fine fraction, and V_{ss} is the volume of the sand particle. Figure 3 shows the relationship between the skeleton void ratio and the fine fraction content after consolidating the soil sample of each fine fraction content with a confining pressure of 98.1 kPa. The skeleton void ratio increases with the fine fraction content (Fc) and shows a value nearly equal to the maximum interstitial ratio e_{max} of Fc = 0% free soil around the fine fraction content Fc = 24%. In this state, it can be said that the interlocking effect of sand particles is lost and very loose. Furthermore, it is considered that the skeletal structure of sand is lost at a fine fraction content beyond that, and the strength of the specimen is controlled by the fine fraction content.

3 RESULTS AND DISCUSSIONS

Figure 4 (i), (ii) show effective stress path for each condition (SF=0% and SF=1%: L=40mm) results from the undrained cyclic shear test. Further, (a), (b) and (c) show the results of fine fraction content Fc = 7%, 21% and Fc = 49%, respectively.

The influence of the fine fraction content appears in each effective stress path and it is understood that the undrained cyclic resistance until liquefaction state is different. These stress path indicate that cycle resistance decrease due to increase of fine fraction content of material until Fc=21%. However, when the skeleton void ratio exceeds Fc = 21%, which exceeds the maximum void ratio of decomposed granite (Figure 3), the number of cycles until liquefaction increases again. In addition, with the increase in fine fraction content, the effective stress of the specimen is not completely disappeared and it has reached a liquefied state due to deformation. This is probably because the skeleton void ratio of specimen shifted from sand to fine grain-based structure. Undrained shear behavior of the soil sample containing the low plasticity fine grain used in this study was found to be strongly influenced by the fine fraction content.

On the other hand, in the case of SF=1 % (L=40mm), resistance for the undrained cyclic shear increases with each condition clearly as same as SF= 0 %. This is attributed to be due to the fact that short fiber inhibit deformation and shear resistance increases by mixing short fiber.

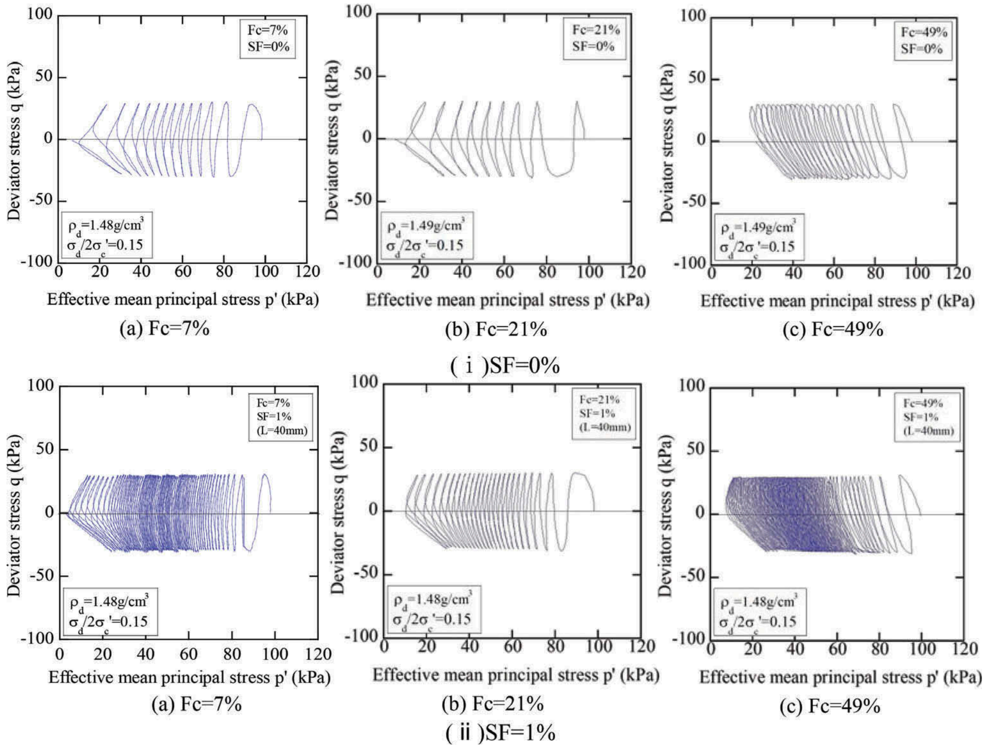

Figure 4. Effective stress paths on undrained cyclic shear behavior (SF=0%, SF=1%).

Figure 5 (i), (ii) shows relationship between axial strain and deviator stress (SF=0% and SF=1%: L=40mm). Further, (a), (b) and (c) show the results of fine fraction content Fc = 7%, 21% and Fc = 49%, respectively.

In the case of SF= 0 %, the strain amplitude suddenly increased and the specimens failed within a few cycles, reaching DA=5 %. Even under undrained cyclic deformation behavior, it is influenced by low-plasticity fine grain particles. As the fine fraction content increases from 21% to 49%, it can be seen that the amount of deformation on the tensile side accompanying cyclic loading decreases.

On the other hand, it is confirmed that by mixing short fiber (SF=1%), the cyclic shear resistance is increased, and deformation on the extension side of the specimen reaching the liquefied state is suppressed. These data indicate that constraint effect is generated by mixing of short fiber, and the rigidity of the specimen increases, so that generation of axial strain is suppressed.

Figure 6 shows relationship between number of cycles and maximum pore pressure ratio for the same cyclic shear stress ratio ($\sigma_d/2\sigma_c' = 0.15$, Fc=21%). In the case of SF=0%, a large excess pore water pressure is generated at the initial stage of cyclic shearing. On the other hand, when short fiber are mixed, the maximum pore water pressure due to cyclic shearing shows a slow generation behavior. These data show that mixing of short fiber suppresses generation of excess pore water pressure. In addition, it can be understood that the excess pore water pressure ratio does not reach 1.0 and it is liquefied due to the influence of fiber length.

Figure 7 shows the relationships between number of cycles and double amplitude axial strain. Double amplitude axial strain gradually increased with increase number of cycles. It can be confirmed that the generation behavior of both amplitude axis strains largely depends on the generation behavior of excess pore water pressure shown in Figure 6. In addition, it can be seen that both results are affected by the length of the short fiber and show generation behavior similar to the generation behavior of the excess pore water pressure.

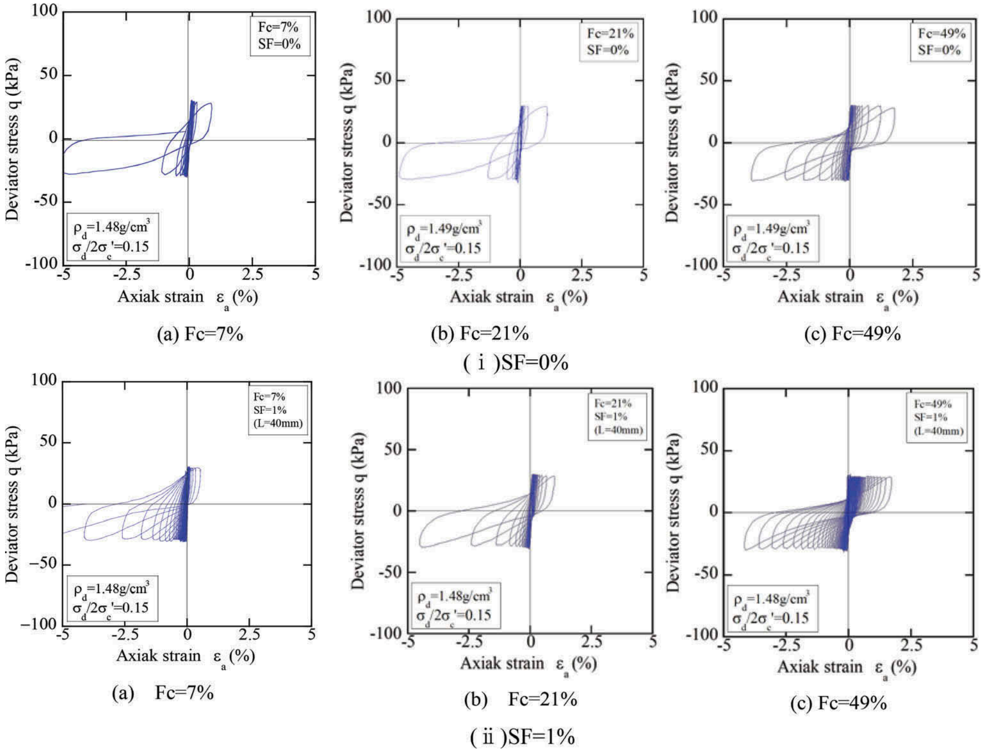

Figure 5. Relationship between axial strain and deviator stress.

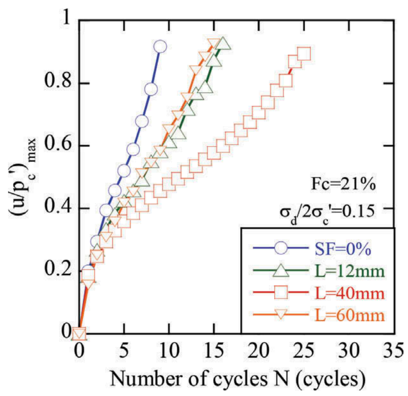

Figure 6. The relationships between number of cycles and maximum pore pressure ratio.

For the case of SF=1 %, the number of cycle increases, and the development of axial strain is suppressed in comparison with SF=0 %. These data indicate that the development of strain effectively suppresses with number of cycle by mixing short fiber. Moreover, the development behavior of double amplitude axial strains is influenced by the length of short fiber, and it is understood that there is the most deformation suppression effect at L=40 mm. This is considered to be due to the fact that the non-uniform state of the short fiber in the specimen occurred due to the relationship between the specimen diameter and the length of the short fiber.

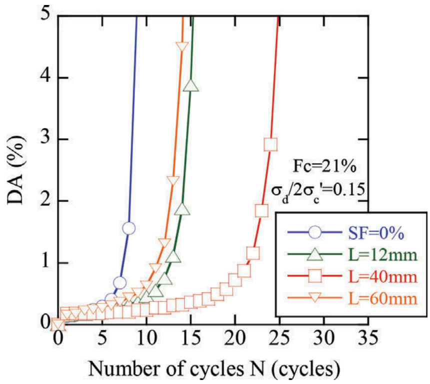

Figure 7. The relationships between number of cycles and double amplitude axial strain.

Figure 8 (a) - (d) shows the liquefaction strength curve for each condition result. For this study, we assumed that liquefaction occurs at DA=5 %. Focusing on the liquefaction strength N_L=20, the liquefaction strength decreases with increase of fine fraction content until Fc=21%. As the skeleton void ratio varies, slight liquefaction strength increases at Fc=21% or more. On the other hands, the liquefaction strength is increased by short fiber mixture. The results of similar tests with short fiber length L of 40 and 60 mm are shown in (c) and (d), respectively. It was revealed that liquefaction strength increases even if the fiber length is increased from 12 to 60 mm. However, under this condition, liquefaction resistance increased most when mixing fiber length L=40 mm. This is considered to be due to the entanglement of the soil particles and the fiber being reduced by setting the fiber length L=60 mm to the specimen diameter of 75 mm at the same fiber amount.

Figure 9 shows the relationship between the liquefaction strength and fine fraction content of short fiber non-mixed soil (SF=0%) and short fiber mixed soil (SF=1%) at each fine fraction content. Here, the liquefaction strength is defined as the repetitive stress ratio at the

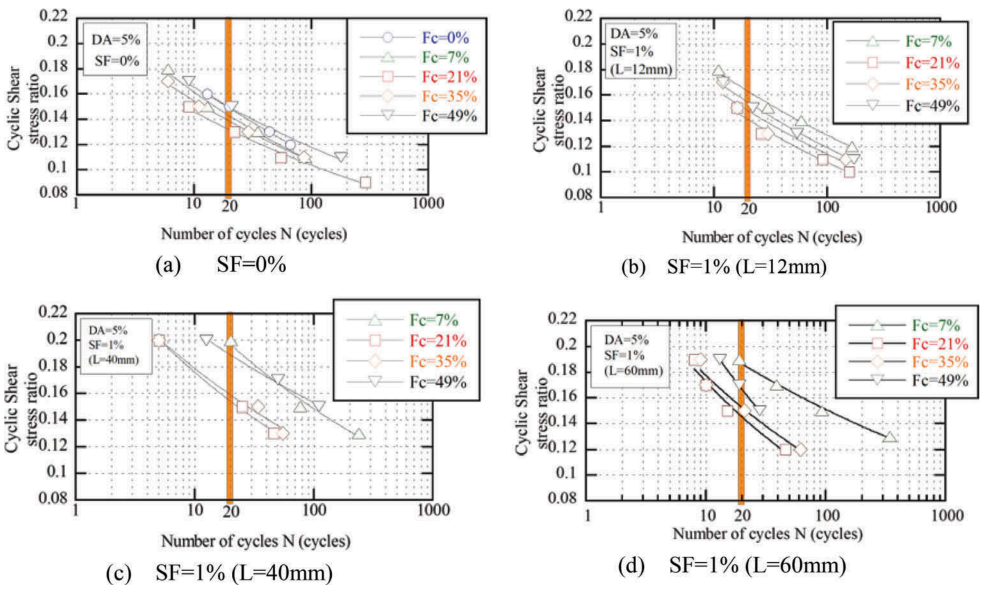

Figure 8. Liquefaction strength curve.

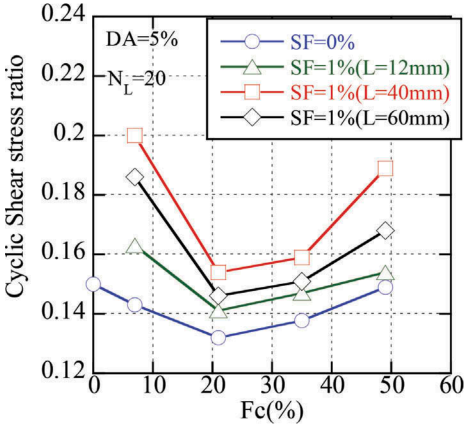

Figure 9. Relationship between Liquefaction strength and fine fraction content Fc.

number of repetitions N_L=20 times at liquefaction determination. The liquefaction strength of the soil containing the low plasticity fine grain is influenced by the skeletal void ratio and causes intensity variation at the fine grain content rate showing the maximum void ratio e_{max} of Fc=0% (Figure 3). In addition, its behaviour is also similar to the feature of fine fraction content even in short fiber mixed soil. Moreover, it became clear that the effect of improving the strength of liquefaction becomes remarkable when the short fiber length becomes long. In particular, when mixing fiber having a fiber length L=40 mm, it can be confirmed that the liquefaction strength is highest at any of the fine fraction content. It is also found that there is a short fiber length most suitable for improvement in the diameter of the specimen.

4 CONCLUSIONS

1. Undrained cyclic shear behavior of soil containing the low plasticity fine fraction largely depends on the change in the skeletal void ratio e_s. Undrained cyclic shear resistance of soil containing the low plasticity fine fraction increases and decreases with the fine fraction content at which the skeleton void ratio and the maximum void ratio become equal to each other as a threshold value.
2. The liquefaction strength of sand containing low plasticity fine fraction is increased by mixing short fiber. It was also confirmed that there is a short fiber length optimum for the improvement effect. Therefore, short fiber mixed soil is one of the useful methods of suppression of liquefaction.

REFERENCES

Costal Development Institute of Technology, 2003, The Premixing Method : Principal, Design and Construction, CRC Press.

Hirano, T., Yoshida, N., Dabashi, K., Fujii, F., and Kanazawa, S., 2013, Mechanical Properties of Fiber Mixed Reinforced Soil, Japan Chapter of International Geosynthetics Society, A1, 28(4), 135-142 (in Japanese).

Ibraim, E., Diambra, A., Muir Wood, D. and Russell, A.R., 2010, Static Liquefaction of Fiber Reinforced Sand under Monotonic Loading, Geotextiles and Geomembranes, 28, 374-385.

Li,H. and Senteakis, 2017, Dynamic Properties of Polypropylene Fiber-Reinforced Silica Quarry Sand, Soil Dynamics and Earthquake Engineering, 100, 224-232.

Miwa, S., Tsutsui, H., Motoyama, H., Ikeda, T., and Numata, A., 2012. Reconnaissance Report on Liquefaction in Kanto Region During the 2011 Tohoku-Chihou Taiheiyo-Oki Earthquake, Journal of Japan Society of Civil Engineers, A1, 68(4), 1250-1265 (in Japanese).

Muir Wood, D., Diambra, A. and Ibraim, E., 2016, Fibers and Soils: A Route Towards Modelling of Root-Soil Systems, Soils and Foundations, 56(5), pp.765-778.
Nakamichi, M., Sato, K., Fujikawa, T., and Koga, C., 2013. Experimental Discussion About Suppressing Liquefaction Using Short Fiber Composite Soil, Geosynthetics Engineering Journal, 28, 55-160 (in Japanese).
Yajima, J., Numata, Y. and Nakane, I., 1996. A Study on Liquefaction Strength Evaluation Methods and Liquefaction Properties of Containing Sand, Journal of Japan Society of Civil Engineers, 624(III-47), 113-122 (in Japanese).
Yasuda, S., Harada, K., Ishikawa, K. and Kanemaru, Y., 2012. Characteristics of Liquefaction in Tokyo Bay area by 2011 Great East Japan Earthquake, Soils and Foundations, 52(5), 793-810.
Zen, K., Yamasaki, H. and Sato, Y., 1990. Strength and Deformation Characteristics of Cement Treated Sands Used for Premixing Method, Report of the Port and Harbour Research Institute, 29(2), 86-117 (in Japanese).